Are small-scale field aligned currents and magnetosheath-like particle precipitation signatures of the same low altitude cusp?

Jürgen Watermann, P. Stauning, H. Lühr, P. T. Newell, F. Christiansen, K. Schlegel

Watermann, J., Lühr, H., Newell, P.T., Christiansen, F., Schlegel, K. (2009): Are small-scale field-aligned currents and magnetosheath-like particle precipitation signatures of the same low-altitude cusp?. - Advances in Space Research, 43, 1, 41-46

DOI: 10.1016/j.asr.2008.03.031

Are small-scale field-aligned currents and magnetosheath-like particle precipitation signatures of the same low-altitude cusp?

J. Watermann [a] P. Stauning [a] H. Lühr [b] P.T. Newell [c]
F. Christiansen [d] K. Schlegel [e]

[a] *Le Studium, 3D avenue de la Recherche Scientifique, F-45071 Orléans cedex 2, France*

[b] *GeoForschungsZentrum Potsdam, Telegrafenberg A 17, D-14473 Potsdam, Germany*

[c] *Applied Physics Laboratory, Johns Hopkins University, 1100 Johns Hopkins Road, Laurel, Maryland 20723 MD, USA*

[d] *Danish National Space Center, Juliane Maries Vej 30, DK-2100 Copenhagen, Denmark*

[e] *Max-Planck-Institute for Solar System Research, Max-Planck-Str. 2, D-37191 Katlenburg-Lindau, Germany*

Abstract

We examined some 75 observations from the low altitude Earth orbiting DMSP, Ørsted and CHAMP satellites which were taken in the region of the nominal cusp. Our objective was to determine whether the actually observed cusp locations as inferred from magnetosheath-like particle precipitation ("particle cusp") and intense small-scale magnetic field variations ("current cusp"), respectively, were identical and were consistent with the statistically expected latitude of the cusp derived from a huge number of charged particle spectrograms ("statistical cusp").

The geocentric coordinates of the satellites were converted into AACGM coordinates, and the geomagnetic latitude of the cusp boundaries (as indicated by precipitating particles and small-scale field-aligned currents) set in relation to the IMF-B_z dependent latitude of the equatorward boundary of the statistical cusp.

We find that the actually observed latitude of the particle cusp matches well the statistically expected latitude while the current cusp appears to cover most of the statistical cusp and also a $\approx 1^\circ$wide section beyond the equatorward boundary of the statistical cusp. This leads us to suggest that intense small-scale field-aligned currents are generated in the cusp but also in the transition zone between the low-latitude boundary layer (LLBL) and the cusp, probably within both regimes, the cusp and the open LLBL. The small-scale field-aligned currents are possibly a consequence of turbulence and/or instabilities associated with the process of opening

previously closed magnetospheric field lines and merging them with the interplanetary magnetic field.

Key words: polar ionosphere, low-altitude cusp, field-aligned currents, charged particle precipitation

1 Introduction

In this paper we compare in detail the cusp latitude inferred from two different ionospheric signatures, namely the occurrence of magnetosheath-like particle precipitation and of intense small-scale magnetic field perturbations indicating small-scale field-aligned currents (FAC).

The average location of the low-altitude cusp was mapped by Newell and Meng (1988) from the analysis of a huge number of spectra of precipitating ions and electrons supposedly originating in the magnetosheath. They used particle spectrometer data which had been collected by various DMSP satellites over a time span of several years. Identification of the cusp in this manner is based on the assumption that intensity and energy distributions of precipitating particles in the cusp region resemble the magnetosheath plasma population more than in any other region of the magnetosphere (Newell and Meng, 1988). We refer to the cusp identified in this way as the "statistical cusp".

Newell et al. (1989) derived a quantitative relation between the magnitude of the IMF-B_z component and the most probable equatorward boundary of the statistical cusp. This "statistical cusp equatorward boundary" defines the reference latitude against which we compare our observations from individual DMSP, Ørsted and CHAMP cusp passes.

The DMSP satellites fly in a high-inclination sun-synchronous circular orbit at some 850 km altitude above the ground. The Ørsted satellites possesses a slowly precessing high inclination elliptic orbit with about 620 km and 860 km perigee and apogee, respectively. The CHAMP satellite follows a circular high inclination orbit. Its local time changes by one hour every 11 days. At the time we took our measurements, CHAMP was about 425 km above the ground; in general its altitude is decaying slowly by some 20 km per year.

Recently it was discovered that large and highly localised magnetic field perturbations with scale sizes ranging from several hundred meters up to a few kilometers are frequently observed in or near the nominal cusp region (Stauning et al., 2003; Neubert and Christiansen, 2003; Watermann et al., 2004). They are indicative of a locally confined zone of high FAC intensity of small spatial scale and map out a region which approximately overlaps the statistical cusp.

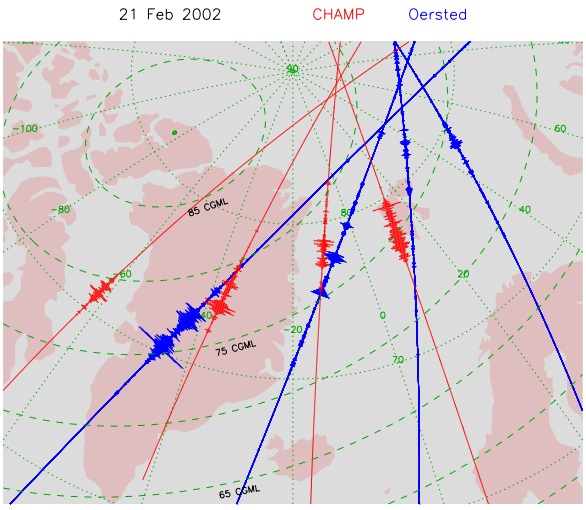

Fig. 1. Small-scale magnetic field variations and FAC, with relative magnitudes indicated by the lengths of the bars across the satellite trajectories. Blue: high-frequency (0.5-25 Hz) $|\delta B|$ residual from Ørsted CSC measurements; red: high-frequency (1-50 Hz) $|j_{||}|$ derived from CHAMP magnetometer data.

In this paper we conduct a more detailed study of DMSP, Ørsted and CHAMP measurements with the objective to gain or loose support for the hypothesis that the low-altitude cusp is characterized by very intense small-scale FAC.

Fig. 1 shows as an example an overlay of small-scale magnetic field fluctuations and FAC derived from data taken during four Ørsted and four CHAMP passes, respectively, over the North Atlantic and Greenland. The intensities are indicated by the length of the bars across the trajectories. High intensities are observed between about 74°and 80°altitude adjusted corrected geomagnetic (AACGM) latitude in the time interval 11.4 to 14.0 magnetic local time (MLT) with the highest intensities seen between 75°and 78°AACGM and 11.7 and 12.2 MLT.

A detailed examination of data from 21 Feb 2002 was documented by Watermann et al. (2004) who considered in addition to the satellite measurements cusp signatures obtained with the Sondrestrom and Svalbard incoherent scatter radars. Their extensive analysis supports the idea that intense small-scale FAC are a signature of the cusp and the open part of the low-latitude boundary layer.

For the present paper we studied some 75 cases of cusp observation collected from the DMSP, Ørsted and CHAMP satellites during the first SIRCUS campaign, February 16-22, 2002. SIRCUS is the acronym for a multi-instrument observational program which focusses on a detailed investigation into the properties and dynamics of the low-altitude cusp. More information on SIRCUS objectives and activities were documented by The SIRCUS Science Team (2003).

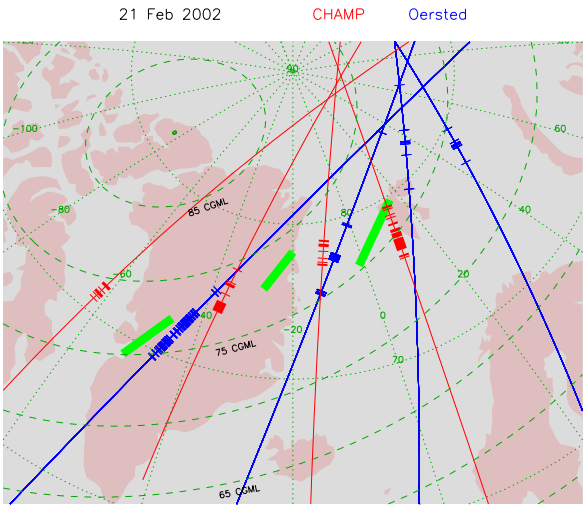

Fig. 2. blue: high-frequency (0.5-25 Hz) $|\delta B|$ residual from Ørsted CSC measurements in excess of 15 nT (wide trajectory segments) and below 15 nT (narrow segments); red: high-frequency (1-50 Hz) $|j_{||}|$ inferred from CHAMP magnetometer data in excess of 20 μA m^{-2} (wide segments) and below 20 μA m^{-2} (narrow segments); green: cusp particle precipitation according to DMSP–F13, –F14 and –F15 observations.

About one third of the cusp crossings examined were inferred from DMSP-F13, -F14 and -F15 particle spectrometer data (termed "particle cusp"), one third from small-scale magnetic field observations made onboard the Ørsted satellite, and one third from CHAMP measurements (the latter two are termed "current cusp").

We shall point out that our definitions of "statistical cusp" and "particle cusp" build on the same physical quantities, namely the spectral characteristics of charged particle precipitation. The difference is merely that the term "statistical cusp" refers to the average or statistically expected particle cusp location as defined by Newell and Meng (1988) while the term "particle cusp" refers to an individual satellite pass where the actually observed cusp location can deviate from the statistically expected location.

2 Space Environment

Solar wind conditions were largely normal during the first SIRCUS campaign. According to ACE measurements, the solar wind velocity fluctuated between 350 and 450 km s^{-1} and the density between 5 and 10 H$^+$ cm^{-3}. The interplanetary magnetic field (IMF) was moderately strong, and its x– , y– and z–components (in GSM coordinates) fluctuated between -7 and +8, -9 and +9, and -5 and +7 nT, respectively. For reference, ACE level-2 solar wind and IMF data of the time interval under consideration were displayed in The

SIRCUS Science Team (2003). The variation of the IMF-B_z component during the (daytime) campaign hours is seen in Fig. 3. The high-latitude geomagnetic field remained rather quiet during the campaign interval according to observations from the Greenland magnetometer chain which indicated that we were not exposed to strong variations of the large-scale ionospheric current system.

Although the interplanetary plasma parameters fluctuated only moderately, the variations of the IMF-B_y and -B_z components are expected to result in detectable shifts of the cusp location – in magnetic local time as well as in magnetic latitude – in accordance with established statistical results (Newell and Meng, 1988; Newell et al., 1989; Aparicio et al., 1991). In this paper we take the IMF-B_z dependence into account and use it to normalize the latitude when comparing individually observed and statistically expected cusp locations.

3 Analysis Method

Since we are concerned with cusp observations we consider only daytime satellite passes. The SIRCUS campaign built on coincident satellite and incoherent scatter radar measurements, therefore the geographic area of the observations was constrained by the field-of-view of the EISCAT Incoherent Scatter Radars at Tromsø and on Svalbard and the Sondrestrom (Greenland) Incoherent Scatter Radar. In consequence we restricted our satellite campaign hours to the 07–16 UT interval.

Small-scale magnetic field variations (in the 0.5–25 Hz range) were tagged as being "present" during a northern hemisphere daytime pass of the Ørsted satellite if they exceeded 15 nT amplitude, and otherwise "absent". Similarly, small-scale field-aligned currents (1–50 Hz) inferred from CHAMP magnetometer measurements were tagged as being "present" if they exceeded 20 μA m^{-2}, and otherwise "absent", see Fig. 2.

For each time interval marked "present" we computed the expected latitude of the statistical equatorward boundary of the cusp according to Newell et al. (1989), using smoothed ACE level-2 IMF data taken one hour prior to the satellite observations. A delay of one hour is appropriate given the average solar wind speed prevailing during the campaign hours. Fig. 3 shows ACE level-2 data from the campaign hours (bottom panel) and the expected equatorward boundary of the statistical cusp (top panel, black line) together with the AACGM latitudes of the observed particle and current cusps (green, blue and red bars, respectively).

In the next step, the geocentric latitude, longitude and altitude parameters

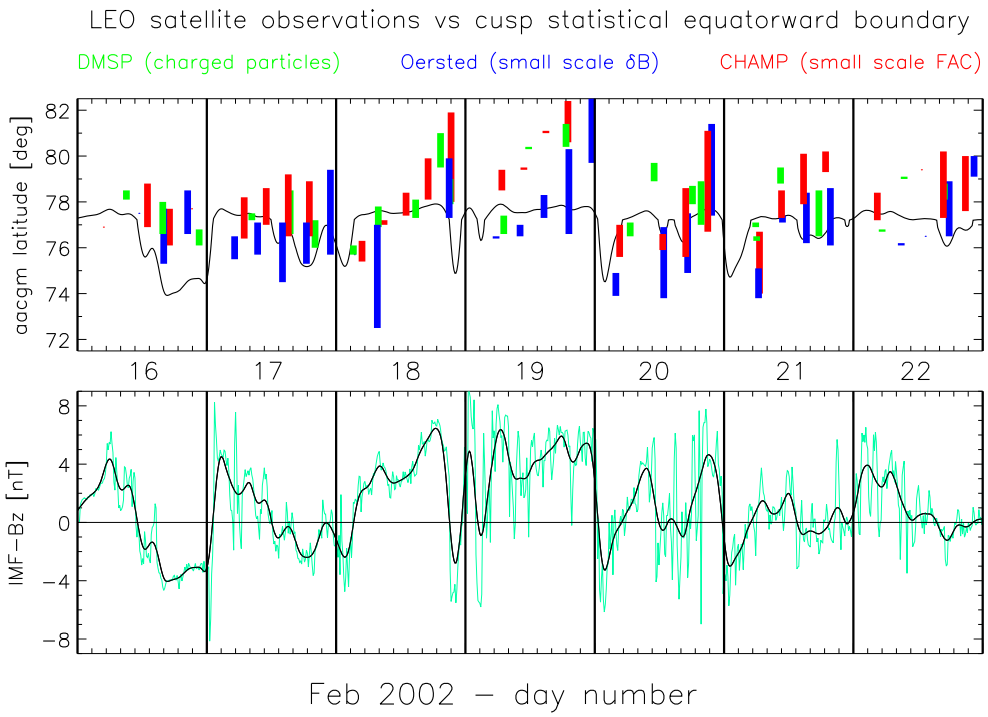

Fig. 3. bottom panel: variation during the seven campaign days from 07 through 16 UT every day, showing 4-min (green) and smoothed (black)data; top panel: statistical equatorward boundary of the cusp (black line), latitudinal extent of the DMSP particle cusp (green bars), the Ørsted small-scale $|\delta B|$ residuals (blue bars) and the CHAMP small-scale $|j_{||}|$ region (red bars). Note that IMF data are advanced by one hour relative to the time of the satellite passes.

of each satellite trajectory which fell into the campaign hours were converted into AACGM coordinates (a system grown out of a combination of CGM and PACE coordinates, see Baker and Wing (1989) and Gustafsson et al. (1992)).

The AACGM latitude difference between the observed equatorward boundary of each "δB present" respectively "$j_{||}$ present" interval and the equatorward boundary of the statistical cusp was then determined. The median value and mean absolute deviation of these differences obtained over the entire campaign interval were then computed.

The procedure was repeated with the observed poleward boundaries of "δB present" and "$j_{||}$ present", respectively, and the equatorward boundary of the statistical cusp in order to compute the difference between the observed poleward boundary of the current cusp and the equatorward boundary of the statistical cusp. Note that a quantitative relation between IMF parameters and the latitude of the statistical cusp was only published for the equatorward boundary but not for the poleward boundary.

The same procedure was applied to the actually observed and the statisti-

Table 1
Differences between mean equatorward and poleward boundaries of the particle cusp and current cusp, respectively, and the equatorward boundary of the statistical cusp

particle cusp equatorward boundary	
– statistical cusp equatorward boundary	0.4°±1.1°
particle cusp poleward boundary	
– statistical cusp equatorward boundary	1.6°±1.2°
Ørsted current cusp equatorward boundary	
– statistical cusp equatorward boundary	-1.0°±1.2°
Ørsted current cusp poleward boundary	
– statistical cusp equatorward boundary	0.6°±1.7°
CHAMP current cusp equatorward boundary	
– statistical cusp equatorward boundary	0.3°±1.3°
CHAMP current cusp poleward boundary	
– statistical cusp equatorward boundary	2.1°±1.4°

cally expected equatorward boundaries of the particle cusp and to the actually observed poleward boundary and the statistically expected equatorward boundary of the particle cusp. The results from all of these computations are displayed in Fig. 4.

4 Analysis Results

The comparison between the equatorward and poleward boundaries of the particle cusp and the current cusp, respectively, on one hand, and the equatorward boundary of the statistical cusp on the other, render the numbers listed in Table 1.

Fig. 4 and Table 1 can be condensed into the following main statements. The particle cusp inferred from DMSP and the current cusp inferred from CHAMP appear to be observed slightly poleward of the statistical cusp, but the differences is small compared with the statistical uncertainty and is insignificant. The current cusp inferred from Ørsted appears to be approximately centered on the equatorward boundary of the statistical cusp which is consistent with the results of Stauning et al. (2003).

Our numbers seem to indicate that the observed current cusp is typically wider than the particle cusp, 1.8°and 1.6°(Ørsted and CHAMP, respectively) versus

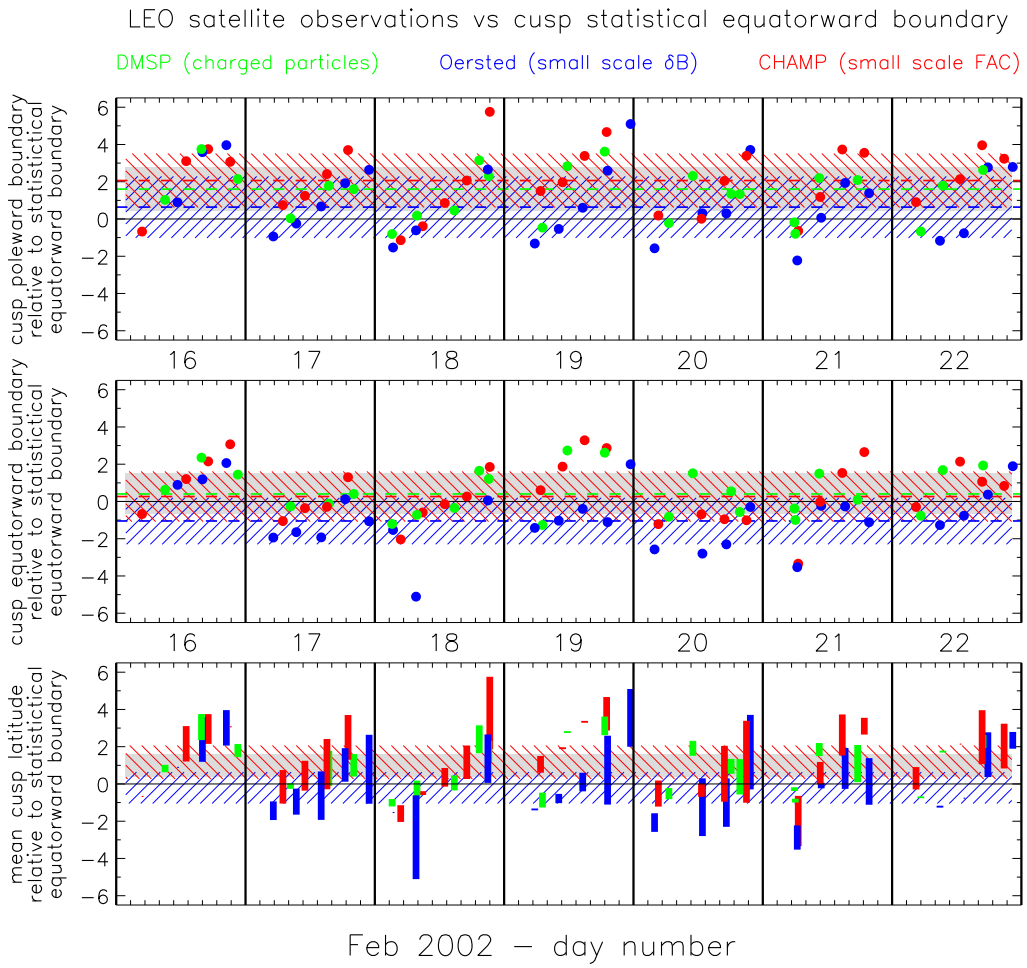

Fig. 4. top panel: difference between observed poleward and statistically expected equatorward boundary of the cusp from DMSP (green), Ørsted (blue) and CHAMP (red) measurements, together with the medians and mean absolute deviations of these differences (solid gray, hatched blue and hatched red areas, resp.); center panel: the same for the difference between observed and statistically expected cusp equatorward boundaries; bottom panel: mean latitudinal extent of the particle cusp (solid gray) and small-scale $|\delta B|$ resp. $|j_{||}|$ variations (hatched blue and hatched red, resp.) together with individual latitudinal cusp spans (blue, red and green bars representing the Ørsted, CHAMP and DMSP satellites). Full hours ranging from 07 through 16 UT every day are indicated by tick marks.

1.2°(DMSP). But that is not a valid conclusion and not necessarily a physical fact. We have set our thresholds for high intensity (15 nT and 20 μA m^{-2}, respectively) based on a reasonable but still arbitrary distinction between low and high intensity, and we have fixed our threshold numbers before computing the statistics. Increasing the threshold will undoubtedly result in an apparently narrower current cusp, and vice versa.

Fig. 4 indicates a tendency of the cusp latitude to increase systematically every day from the begin to the end of the time interval under consideration (07 to

16 UT). This is a manifestation of the dipole tilt angle effect on the average cusp latitude. As seen in Fig. 1 and Fig. 2 (whose geographical coverage is representative for all seven campaign days) the dipole tilt angle decreases from early campaign hours (magnetic noon east of Svalbard) to late campaign hours (magnetic noon west of Greenland).

The tilt angle dependence of the location of the low-altitude cusp was investigated by Newell and Meng (1989). They conclude that the cusp decreases by about 0.06°in magnetic latitude for each degree increase in dipole tilt angle. This effect is most significant on a seasonal scale but also apparent on a diurnal scale. The physical explanation lies in the tilt angle dependent asymmetry of the magnetopause and magnetotail current systems and the difference in electric conductivity between the dark and the sunlit ionosphere. It would therefore make sense to expand the study and consider many more cusp crossings such that data subsets can be formed which are binned according to the dipole tilt angle.

We were surprised to observe a small but systematic difference between the current cusp latitudes inferred from CHAMP and Ørsted magnetic field measurements, respectively. The satellite altitude difference cannot account for it since we converted all positioning information into AACGM coordinates – and the difference in altitude was only between 200 and 400 km anyway. Such a difference has a negligible effect on the calculation of the geomagnetic coordinates since the magnetic field is almost vertical at these high magnetic latitudes. The puzzle remains unsolved for the time being and awaits further investigations.

It is somewhat confusing to note that the current cusp inferred from CHAMP magnetometer data coincides well with the particle cusp inferred from DMSP particle data while the current cusp inferred from Ørsted measurements appears to straddle the statistical cusp equatorward boundary. We do not consider it unlikely that particle cusp and current cusp do not perfectly overlap since they represent different physical parameters and mechanisms.

5 Conclusions

During the February 2002 SIRCUS campaign, which took place under relatively quiet interplanetary and magnetospheric conditions, nearly coincident data of low-energy charged particle precipitation recorded by the DMSP-F13, -F14 and -F15 satellites, intense small-scale (0.5-25 Hz) magnetic field variations measured by the Ørsted satellite and intense small-scale (1-50 Hz) field-aligned currents inferred from CHAMP magnetometer observations were collected. They were examined with the objective to identify and map the low-

altitude cusp in the northern hemisphere. From a limited statistical sample consisting of 25 charged particle spectra, 24 small-scale δB and 28 small-scale $j_{||}$ observations we obtained the following results.

Intense small-scale magnetic field variations resp. field-aligned currents (FAC) were observed in the particle cusp but also on its equatorward side. The latter represents probably the poleward section of the low-latitude boundary layer (LLBL) which is considered to contain newly opened geomagnetic field lines. The small-scale FAC are possibly a consequence of turbulence and instabilities associated with the process of opening previously closed magnetospheric field lines and merging them with the interplanetary magnetic field. We therefore suggest that intense small-scale FAC are a characteristic signature of the cusp and the open part of the LLBL, i.e., they are not a unique feature of the low-altitude cusp in a strict sense. Since our observations were taken under quiet conditions it seems unlikely that highly variable magnetospheric dynamics have resulted in rapidly changing conditions which could introduce a significant temporal variability to the cusp location. Under very disturbed conditions a direct comparison between data from different satellites would be subject to larger uncertainties unless the measurements were taken truly simultaneously.

Acknowledgement: ACE level 2 data were kindly provided by the ACE Science Center at CalTech. The Ørsted satellite is operated by TERMA Electronics and the Danish Meteorological Institute (DMI), and the data were processed by the Ørsted Science Data Center at DMI. The Ørsted vector magnetometer and star imager were built at the Ørsted·DTU Institute at the Danish Technical University. The Ørsted satellite project is funded by the Danish Ministry of Transport, the Ministry of Research and Information Technology, the Ministry of Trade and Industry, and the Danish Research Councils. The CHAMP satellite project is managed by the GFZ Potsdam with financial and operational support from the Federal Ministry of Education and Research, the GFZ Potsdam and the German Aerospace Center (DLR).

References

Aparicio, B., Thelin, B., and Lundin, R.: The polar cusp from a particle point of view: A statistical study based on Viking data, J. Geophys. Res., 96, 14,023–14,031, 1991.

Baker, K. B. and Wing, S.: A new magnetic system for conjugate studies at high latitude, J. Geophys. Res., 94, 9139–9143, 1989.

Gustafsson, G., Papitashvili, N., and Papitashvili, V.: A revised corrected geomagnetic coordinate system for Epochs 1985 and 1990, J. Atmos. Terr. Phys., 54, 1609–1631, 1992.

Neubert, T. and Christiansen, F.: Small-scale, field-aligned currents at the topside ionosphere, Geophys. Res. Lett., 30(19), doi:10.1029/2003GL017 808, 2003.

Newell, P. and Meng, C.-I.: The cusp and the cleft/boundary layer: Low-altitude identification and statistical local time variation, J. Geophys. Res., 93, 14,549–14,556, 1988.

Newell, P., and Meng, C.-I.: Dipole tilt angle effects on the latitude of the cusp and cleft/low-latitude boundary layer, J. Geophys. Res., 94, 6949–6953, 1989.

Newell, P., Meng, C.-I., Sibeck, D., and Lepping, R.: Some low-altitude cusp dependencies on the interplanetary magnetic field, J. Geophys. Res., 94, 8921–8927, 1989.

Stauning, P., Primdahl, F., Christiansen, F., and Watermann, J.: Detection of high-latitude fine-scale field-aligned current structures from the Ørsted satellite, in OIST-4 Proceedings, edited by P. S. et al., DMI Scientific Report 03-09, ISSN 0905-3263, ISBN 87-7478-484-6, pp. 167–174, 2003.

The SIRCUS Science Team: SIRCUS Workshop Report (compiled by J. Watermann), in OIST-4 Proceedings, edited by P. Stauning et al., DMI Scientific Report 03-09, ISSN 0905-3263, ISBN 87-7478-484-6, pp. 327–334, 2003.

Watermann, J., Lühr, H., Schlegel, K., Stauning, P., Thayer, J., Christiansen, F., and Newell, P.: The low-altitude cusp: multi-point observations during the February 2002 SIRCUS campaign, in Earth Observation with CHAMP: Results from Three Years in Orbit, edited by C. Reigber, H. Lühr, P. Schwintzer, and J. Wickert, pp. 366–372, Springer-Verlag Berlin Heidelberg New York, 2004.